The Journal of Clinical Endocrinology & Metabolism, 2022, **107**, 3328–3340
https://doi.org/10.1210/clinem/dgac528
Advance access publication 9 September 2022
Clinical Research Article

Premature Ovarian Insufficiency in CLPB Deficiency: Transcriptomic, Proteomic and Phenotypic Insights

Elena J. Tucker,[1,2] Megan J. Baker,[3,4] Daniella H. Hock,[3,4] Julia T. Warren,[5] Sylvie Jaillard,[6,7] Katrina M. Bell,[1] Rajini Sreenivasan,[1,2] Shabnam Bakhshalizadeh,[1,2] Chloe A. Hanna,[1,2,8] Nikeisha J. Caruana,[3,4,9] Saskia B. Wortmann,[10,11] Shamima Rahman,[12] Robert D. S. Pitceathly,[13] Jean Donadieu,[14,15,16] Aurelia Alimi,[14,15,16] Vincent Launay,[17] Paul Coppo,[18] Sophie Christin-Maitre,[19] Gorjana Robevska,[1] Jocelyn van den Bergen,[1] Brianna L. Kline,[1] Katie L. Ayers,[1,2] Phoebe N. Stewart,[20] David A. Stroud,[1,3,4] Diana Stojanovski,[3,4] and Andrew H. Sinclair[1,2]

[1]Murdoch Children's Research Institute, Royal Children's Hospital, Melbourne, VIC 3052, Australia
[2]Department of Paediatrics, University of Melbourne, Melbourne, VIC 3010, Australia
[3]Department of Biochemistry and Pharmacology, The University of Melbourne, Parkville, VIC 3010, Australia
[4]Bio21 Molecular Science and Biotechnology Institute, The University of Melbourne, Parkville, VIC 3010, Australia
[5]Division of Hematology-Oncology, Department of Pediatrics, Washington University School of Medicine, Saint Louis, MO 63110, USA
[6]Univ Rennes, CHU Rennes, INSERM, EHESP, IRSET (Institut de recherche en santé, environnement et travail)—UMR_S 1085, F-35000 Rennes, France
[7]CHU Rennes, Service de Cytogénétique et Biologie Cellulaire, F-35033 Rennes, France
[8]Department of Gynaecology, The Royal Children's Hospital, Melbourne, VIC 3052, Australia
[9]Institute for Health and Sport (IHES), Victoria University, Melbourne, VIC, 3011, Australia
[10]University Children's Hospital, Paracelsus Medical University (PMU), Salzburg 5020, Austria
[11]Radboud Center for Mitochondrial Medicine, Department of Pediatrics, Amalia Children's Hospital, Radboudumc, Nijmegen 6524, The Netherlands
[12]Mitochondrial Research Group, UCL Great Ormond Street Institute of Child Health, and Metabolic Unit, Great Ormond Street Hospital for Children NHS Foundation Trust, London WC1N 3JH, UK
[13]Department of Neuromuscular Diseases, UCL Queen Square Institute of Neurology and The National Hospital for Neurology and Neurosurgery, London, WC1N 3BG, UK
[14]Sorbonne Université, Service d'Hémato-oncologie Pédiatrique, Assistance Publique-Hopitaux de Paris (AP-HP), Hôpital Trousseau, Paris 75006, France
[15]Registre Français des Neutropénies Congénitales, Hôpital Trousseau, Paris 75006, France
[16]Centre de Référence des Neutropénies Chroniques, AP-HP, Hôpital Trousseau, Paris 75006, France
[17]Hematologie, Centre Hospitalier de St Brieuc, Paris 22027, France
[18]Sorbonne Université, Service d'hématologie Hôpital Saint-Antoine, AP-HP, Paris 75006, France
[19]Sorbonne Université, Service d'Endocrinologie, diabétologie et médecine de la reproduction Hôpital Saint-Antoine, AP-HP, Paris 75006, France
[20]Department of Paediatrics, The Royal Hobart Hospital, Tasmania 7000, Australia

Correspondence: Elena J. Tucker, BSc(Hons), PhD. Murdoch Children's Research Institute, Royal Children's Hospital, 55 Flemington Rd, Parkville, VIC 3052, Australia. Email: elena.tucker@mcri.edu.au.

Abstract

Context: Premature ovarian insufficiency (POI) is a common form of female infertility that usually presents as an isolated condition but can be part of various genetic syndromes. Early diagnosis and treatment of POI can minimize comorbidity and improve health outcomes.

Objective: We aimed to determine the genetic cause of syndromic POI, intellectual disability, neutropenia, and cataracts.

Methods: We performed whole-exome sequencing (WES) followed by functional validation via RT-PCR, RNAseq, and quantitative proteomics, as well as clinical update of previously reported patients with variants in the *caseinolytic peptidase B* (*CLPB*) gene.

Results: We identified causative variants in *CLPB*, encoding a mitochondrial disaggregase. Variants in this gene are known to cause an autosomal recessive syndrome involving 3-methylglutaconic aciduria, neurological dysfunction, cataracts, and neutropenia that is often fatal in childhood; however, there is likely a reporting bias toward severe cases. Using RNAseq and quantitative proteomics we validated causation and gained insight into genotype:phenotype correlation. Clinical follow-up of patients with CLPB deficiency who survived to adulthood identified POI and infertility as a common postpubertal ailment.

Received: 17 June 2022. **Editorial Decision:** 31 August 2022. **Corrected and Typeset:** 5 October 2022

Conclusion: A novel splicing variant is associated with CLPB deficiency in an individual who survived to adulthood. POI is a common feature of postpubertal female individuals with CLPB deficiency. Patients with CLPB deficiency should be referred to pediatric gynecologists/endocrinologists for prompt POI diagnosis and hormone replacement therapy to minimize associated comorbidities.

Key Words: CLPB, premature ovarian insufficiency, genetics, neutropenia, primary mitochondrial disease, mitochondria, infertility

Abbreviations: 3-MGA-uria, 3-methylglutaconic aciduria; ACN, acetonitrile; CLPB, caseinolytic peptidase B; dDIA, direct data-independent acquisition; FSH, follicle-stimulating hormone; HRT, hormone replacement therapy; MAF, minor allele frequency; OXPHOS, oxidative phosphorylation; POI, premature/primary ovarian insufficiency; PTC, premature termination codon; SDS-PAGE, sodium dodecyl sulfate–polyacrylamide gel electrophoresis; UPR^{MT}, mitochondrial unfolded protein response; WES, whole-exome sequencing.

Mitochondria are the main source of eukaryotic cellular energy. Mitochondrial dysfunction is associated with many human pathologies, including mitochondrial diseases, a group of genetic disorders associated with defects in energy production. The integrity of the mitochondrial proteome is protected by quality control mechanisms, such as the mitochondrial unfolded protein response (UPR^{MT}). UPR^{MT} can be activated by stressors such as impaired oxidative phosphorylation, accumulation of misfolded proteins, deletion of mitochondrial DNA, or increased reactive oxygen species (1-3). CLPB is a mitochondrial protein disaggregase proposed to be involved in the UPR^{MT} response (4).

Pathogenic variants in the *CLPB* gene have been linked to an autosomal recessive syndrome involving 3-methylglutaconic aciduria (3-MGA-uria), neurological dysfunction, cataracts and neutropenia that is often fatal in childhood (OMIM 616271). Most patients first described had a severe presentation including progressive encephalopathy, intellectual disability, epilepsy, congenital neutropenia, cataracts, and death in early childhood (5-7). These patients most often had biallelic loss-of-function variants (8). A minority of patients, usually those harboring missense variants, survived childhood, but the long-term health implications of CLPB deficiency are not well established. More recently, dominant-negative heterozygous missense *CLPB* variants affecting the C-terminal ATP-binding domain, have been shown to cause isolated severe congenital neutropenia (9, 10).

Mitochondrial function is known to be critical for female fertility and to have a role in ovarian aging (11). Oocytes have a particularly high energy demand and, reflective of this, are believed to harbor the greatest number of mitochondrial DNA copies of any human cell (12). Not only does ovarian function rely on efficient energy supply, but it also can be disrupted by faulty mitochondria. Oocytes are particularly susceptible to the reactive oxygen species generated by dysfunctional mitochondria (13, 14). Premature/primary ovarian insufficiency (POI) or diminished ovarian reserve are common manifestations of postpubertal female mitochondrial disorders (15). POI is a clinically and genetically heterogeneous condition characterized by loss or absence of ovarian function and elevated follicle stimulating hormone (FSH) before the age of 40. POI not only has an impact on reproductive potential but is also associated with an increased risk of osteoporosis, diabetes, cardiovascular disease, and early mortality, related to estrogen deficiency (16-18).

POI most often presents as an isolated condition but can also be syndromic. The distinction between isolated and syndromic POI, however, can be blurred, with some cases initially diagnosed with isolated POI but evolving into POI-like syndromes as additional symptoms manifest (19, 20). Furthermore, POI is an often-overlooked component of genetic syndromes, for example, only being mentioned in supplementary text or omitted altogether in research publications, likely because amenorrhea causes fewer immediate concerns to patients that have more pertinent health problems. Early genomics studies have a tendency for bias toward severe presentations. As genomic studies become more frequent, the clinical spectrum of patient phenotype is becoming evident. Mildly affected and surviving patients may manifest with unanticipated symptoms. Such symptoms are imperative to recognize because they can influence patient management and ultimately their long-term health and happiness. For example, the prompt treatment of women with POI using hormone replacement therapy (HRT) can minimize the risk of comorbidities such as osteoporosis and heart disease (21, 22). Furthermore, presymptomatic identification of POI opens the possibility of fertility preservation before oocytes are depleted, which may be desired by individuals affected by mild syndromes.

Here we describe the first pathogenic *CLPB* splicing variant in a patient with survival to adulthood. We demonstrate that this variant leads predominately to exon skipping. Via proteomics, we demonstrate a low level of CLPB protein but no decrease in abundance of oxidative phosphorylation (OXPHOS) complexes. We discern the biological impact of CLPB depletion on the proteome of patient lymphoblasts. Via long-term health follow-up on surviving patients, we highlight ovarian dysfunction as a common symptom in postpubertal girls. Prompt recognition of POI in affected individuals will improve patient management and outcomes.

Methods

Participant Description

The patient (AS19D035) was recruited after clinical consultation as part of our ongoing research program investigating the genetics of POI (N = 80 patients with isolated or syndromic POI, to date).

She is currently 18 years of age and has a history of multiple infections, including neonatal pneumonia, recurrent tonsilitis, bronchiolitis, chicken pox, a right cubital fossa abscess, a left knee abscess, right orbital cellulitis, and cervical adenitis before the diagnosis of severe neutropenia (0.1×109/L). Treatment with granulocyte colony-stimulating factor was initiated, leading to normalization of blood parameters. She has myopia and at 3 years of age bilateral cataracts were noticed, with lens replacement performed at 4 years of age. She has intellectual disability with a full-scale intelligence quotient (FSIQ) of 58. She was referred to endocrinology for short stature (2nd percentile, 141.5 cm at 13 years with midparental height of 160.5 cm) and was noted to have delayed puberty. She had primary amenorrhea and breast development at Tanner stage I. Her natural pubic and auxiliary hair development remains unknown, since it was not examined at initial presentation and she has since had pubertal induction/HRT that has likely caused development. Hormonal assessment led to a diagnosis of POI with elevated FSH of 73 IU/L (reference range 1.0–8.0 IU/L)(Table 1). Luteinizing hormone was

Table 1. Clinical update of patients with CLPB deficiency surviving beyond puberty, as well as clinical summary of the prepubertal patient discussed in this manuscript (SCINR-2735) with variants comparable to the primary case study AS19D035)

				Reproductive function			Growth		Bone	Immunological function		Neuro/muscular function	Metabolic		Vision	Heart	Kidney
Patient	Age	Sex	Variants	Amenorrhea/ puberty	Hormones	Imaging	Height	Hormones		Neutropenia/ treatment	Other		Urinary 3-MGA	Mitochondria			
AS19D035 (this study)	18	F	Compound heterozygous c.[1275+ 5G>A];[1249C>T] p.[?];[p.Arg417Ter]	Primary amenorrhea Delayed puberty Tanner stage I breast development	FSH:73 IU/L LH: 16 IU/L Inhibin B <10 ng/L E < 18 pg/mL	U/S: no detectable ovaries, small prepubertal uterus MRI: no detectable ovaries, small prepubertal uterus	Short stature that normalized after pubertal induction	IGF1: 15 (low) IGF BP3: 152 (normal) Glucagon stimulation test: normal	Normal	Congenital (severe) Treated with G-CSF	History of recurrent infection, asthma, eczema	IQ: 58 Normal MRI	Normal	Lb: Normal OXPHOS subunit composition	Bilateral cataracts Myopia	Normal	Normal
#6 PMID: 25597510	26	F	Compound heterozygous c.[1305_1307delinsCCC]; [1937G>T] p.[Glu435_Gly436delins AspPro];[p.Gly646Val]	Secondary amenorrhea (always oligomeric) Normal puberty	FSH: 169 IU/L E < 12pg/mL	Data not available	90th percentile	NR	NR	Chronic (moderate) Not treated	Hypothyroid	IQ: 72 Cerebellar atrophy Ataxia/tremor	Elevated	Fb: Normal OXPHOS activity Muscle: Normal OXPHOS activity	Bilateral congenital cataracts Hyperopia	Normal	Normal
P1 PMID: 25595726	31	F	Compound heterozygous c.[1882C>T];[1915G>A] p. [Arg628Cys]; [Glu639Lys]	Primary amenorrhea Delayed puberty	FSH: 108 IU/L LH: 43.8 E: 115 (HRT)	U/S: Normal uterus Detectable ovaries	Short stature	NR	Normal (2yrs)	No	History of recurrent upper respiratory tract infections	IQ: normal	Elevated	Muscle biopsy: increased lipid deposition, no OXPHOS deficiency CSF and blood: normal lactate	Bilateral congenital cataracts	Normal	Normal
Fr-1502 PMID: 34115842	31	F	Heterozygous c.1682G>A p.Arg561Gln	Primary amenorrhea Delayed puberty	FSH: 57.2 E: 16	U/S: Detectable ovaries of normal morphology	Normal	IGF1: 12 (low)	NR	Congenital (severe) Treated with G-CSF	Recurrent infections	Normal MRI	NR	NR	Bilateral cataracts	Normal	Normal
FR 0038 PMID: 34115842	28	F	Heterozygous c.1682G>A p.Arg561Gln	Primary amenorrhea Delayed puberty	FSH: 33 E: 9	U/S: left ovary not detected, right ovary poorly visualized	Normal after GH replacement from 10 yrs	GH insufficiency	Body:—1.3 SD Spine: −1.1 SD	Congenital (severe) Treated with G-CSF	Recurrent infections	Normal MRI	Normal	NR	Normal	Normal	Normal
[a]SCINR-2735	3	F	Compound heterozygous c.[1249C>T];[1257 +5G>T] p.[Arg417Ter];[?]	NA	NA	NA	NR	NR	NR	Congenital (severe) Treated with G-CSF	Skin infections	NR, no neurological signs	NR	NR	Bilateral cataracts	NR	NR
P2 PMID: 25595726	30	M	Compound heterozygous c.[1882C>T];[1915G>A] p. [Arg628Cys]; [Glu639Lys]	Normal	LHRH stim: Normal TRH stim: Normal	Oligospermia	Normal after GH replacement from 4–16 yrs	GH insufficiency	Spine: −1.5 SD Hip: −1.2 SD	No	Hay fever	IQ: normal	Elevated	NR	Bilateral congenital cataracts Strabismus (surgically treated) Myopia Nystagmus	NR	Nephrocalcinosis, Renal cysts, Right renal calculus
FR 0019 PMID: 34115842	38	M	Heterozygous c.1163C>A p.Thr388Lys	Normal	NR	Azoospermia	Normal	NR	Normal	Agranulocytosis	Recurrent infections	Epilepsy	NR	NR	Normal	NR	NR

Abbreviations: G-CSF, granulocyte colony-stimulating factor; NA, not applicable; NR, not reported; FSH, follicle-stimulating hormone; LH, luteinizing hormone; E, estradiol; GH, growth hormone; OXPHOS, oxidative phosphorylation.
[a]Prepubertal, with reproductive function unknown.

16 U/L, estradiol was < 18 pmol/L and inhibin B was low at < 10 ng/L, indicative of low ovarian reserve (23). Pelvic ultrasound and magnetic resonance imaging (MRI) revealed no detectable ovarian structures and a small prepubertal uterus. Hormone replacement therapy was initiated, and she was 158 cm by age 16 (20th percentile), suggesting that the cause of her short stature was delayed puberty. She had no known family history of POI or infertility, nor of intellectual disability, although her parents and brother had learning difficulties without formal assessment. Available family and medical history are summarized in Table 1.

General Molecular Techniques

Genomic DNA was extracted from EDTA-blood samples by the Victorian Clinical Genetics Service (VCGS). Concentration and integrity were assessed by Qubit dsDNA BR Assay (Thermo Fisher Scientific) and TapeStation (Agilent), respectively. Selected variants were validated by Sanger sequencing using BigDye v3.1 Terminators (Applied Biosystems) and ABI 3130X. Primer sequences are available on request.

Whole-Exome Sequencing

DNA underwent whole-exome sequencing (WES) with SureSelect Human All Exon V6 (Agilent) capture and sequencing on the NovaSeq 6000 (Illumina). All WES data were processed using the Cpipe pipeline (24) and deposited into SeqR for analysis (https://seqr.broadinstitute.org/).

We performed 2 phases of analysis as previously described (25)—the first was gene-centric (POI genes, list available upon request) and the second was an unbiased variant-centric approach. Variant-centric analysis focused on high-priority variants (those considered likely to lead to loss of function: frameshift, nonsense, and splice site variants) in any gene and with any inheritance, or potentially biallelic moderate-high priority variants (missense, in-frame indels, frameshift, nonsense, or splice spite). Only variants with minor allele frequency (MAF) <0.001 in the 1000 Genomes and gnomAD (https://gnomad.broadinstitute.org/) databases and with high quality scores (Q > 50 and allele balance > 25) were considered. Missense variant pathogenicity was predicted in silico using Mutation Taster (http://www.mutationtaster.org/), Polyphen-2 (http://genetics.bwh.harvard.edu/pph2/), SIFT/Provean (http://provean.jcvi.org/), and CADD (Combined Annotation-Dependent Depletion) (https://cadd.gs.washington.edu/snv). The conservation of affected residues was assessed by Multiz Alignments of 100 vertebrates (UCSC Genome Browser https://genome.ucsc.edu/). Described variants were submitted to ClinVar (SCV002515966—SCV002515967).

Reverse Transcription–Polymerase Chain Reaction

RNA was extracted from transformed lymphoblasts using TRIZOL Reagent (Invitrogen) and cDNA was generated using GoScript Reverse Transcription System (Promega) as per manufacturers' protocols. Polymerase chain reaction (PCR) primer sequences available upon request.

RNA Seq

Lymphoblast RNA quality was assessed using TapeStation and 400 ng RNA was used for Illumina TruSeq Stranded mRNA library preparation. Sequencing was performed on the NovaSeq 6000 with 2 × 150 bp reads at depth of ~80 M reads per sample. Raw data were filtered for quality, then trimmed using Cutadept. Reads were aligned to the human genome (GRCh38) using HISAT2 (26). Splicing effects were assessed visually using the Integrative Genomics Viewer8 (Broad Institute, MA) and its in-built Sashimi plot function (27).

Quantitative Proteomics

Primary whole-cell lymphoblast pellets from the patient with biallelic *CLPB* variants (3 replicates from the same individual) and controls (1 replicate from 2 individuals) were solubilized in 5% sodium dodecyl sulfate (SDS), 50 mM tetraethylammonium bromide (TEAB) pH 8.5 and quantified using the Pierce BCA Protein Assay Kit (ThermoFisher Scientific). A total of 25 µg of whole cell protein was isolated and prepared for analysis using Micro S-TRAP columns (PROFITI) according to the manufacturer's instructions. Tryptic digestion was performed (1:25 trypsin to protein ratio). Following elution, samples were dried in a CentriVap Benchtop Vacuum Concentrator (Labconco, Kansas City, MO) and reconstituted in 0.1% trifluoroacetic acid and 2% acetonitrile (ACN) before measurement of peptide concentration. Approximately 1 µg of protein per replicate was loaded on an OrbiTrap Eclipse Mass Spectrometer (Thermo Fisher Scientific) for liquid chromatography–tandem mass spectrometry (LC-MS/MS) analysis. The LC system was equipped with an Acclaim Pepmap nano-trap column (Dionex-C18, 100 Å, 75 µm × 2 cm) and an Acclaim Pepmap RSLC analytical column (Dionex-C18, 100 Å, 75 µm × 50 cm). Tryptic peptides were injected to the enrichment column at an isocratic flow of 5 µL/min of 2% v/v ACN containing 0.1% v/v formic acid for 5 minutes applied before the enrichment column was switched in-line with the analytical column. The eluents were 5% dimethyl sulfoxide (DMSO) in 0.1% v/v formic acid (solvent A) and 5% DMSO in 100% v/v ACN and 0.1% v/v formic acid (solvent B). The flow gradient was (i) 0 to 6 minutes at 3% B; (ii) 6 to 7 minutes, 3% to 4% B; (ii) 7 to 82 minutes, 4% to 25% B; (iii) 82 to 86 minutes, 25% to 40% B; (iv) 86 to 87 minutes, 40% to 80% B; (v) 87 to 90 minutes, 80% B; (vi) 90 to 95 minutes, 80% to 3% and equilibrated at 3% B for 10 minutes before the next sample injection. For data-independent acquisition (DIA) experiments, full MS resolutions were set to 120 000 at m/z and scanning from 350–1400 m/z in the profile mode. Full MS automatic gain control (AGC) target was 250% with an IT of 50 ms. AGC target value for fragment spectra was set at 2000%; 50 windows of 13.7 Da were used with an overlap of 1 Da. Resolution was set to 30 000 and maximum IT to 55 ms. Normalized collision energy was set at 30%. All data were acquired in centroid mode using positive polarity.

Raw data were processed using the Spectronaut platform (version 15.2.210819.50606, Rubin) and searched against the UniProt human database (canonical peptides + isoforms, reviewed, 42 386 entries). The protein report was imported into the Perseus software package (version 1.6.15.0). Briefly, MS2 Quantity outputs for patient and control samples were Log_2-transformed and potential contaminants (eg, keratin) were removed using a curated list. Proteins were annotated using the MitoCarta 3.0 dataset by matching against UniProt ID. Patient and control samples were grouped (patient/control) and proteins with fewer than 2 hits per group were filtered. The whole cell dataset was normalized to the mean using the "subtract" function. For the mitochondrial

complement, all non-mitochondrial proteins were excluded. For both whole cell and mitochondrial datasets, a two-sided Student *t* test was performed with significance determined by *P* value (*P* value < 0.05), displayed as a volcano plot using the scatter plot function in Perseus.

For the relative peptide abundance plot, the "PEP.MS2 Quantity" option was selected in Spectronaut to export the peptide report. CLPB peptides were filtered from "PG.Genes' column and the difference of the means of the Log_2 MS2 intensities from patient and control were calculated for each CLPB peptide. The peptide spanning across amino acids 393–412 was not detected in the patient with *CLPB* variants and further imputed with the lowest value for CLPB peptide in the patient. The difference of the means was plotted using the geom_smooth function of ggplot2 library in RStudio (v. 1.3.1093) which shows a loess smoothed curve with 95% confidence interval. For Relative Complex Abundance (RCA) plot, MS2 intensity from proteins belonging to OXPHOS complexes were plotted in R (RStudio) calculating the difference between the CLPB and control MS2 intensities for each subunit. The mean and standard deviation were then calculated, along with the confidence interval based on the t-statistic for each complex (calculated from the difference between the control and patient samples from each subunit). A paired *t* test calculated significance between the control and patient relative abundances for each complex.

Mitochondrial Isolation

Mitochondria were purified from isolated patient and control lymphoblasts using differential centrifugation as previously described (28). Briefly, cell pellets (5×10^7 cells) were homogenized in mitochondrial isolation buffer (20 mM HEPES-KOH, pH 7.4, 220 mM mannitol, 70 mM sucrose, 1 mM EDTA, 0.5 mM PMSF, 2 mg/mL BSA) and clarified via centrifugation at 800*g* to pellet cellular debris. The residual supernatant was isolated and further clarified at 12 000*g* to obtain an enriched mitochondrial pellet.

SDS-PAGE Immunoblotting Analysis

Tris-Tricine SDS–polyacrylamide gel electrophoresis (SDS-PAGE) was performed as previously described (29). To resolve CLPB processing intermediates, an 8% to 10% gradient Tris-Tricine gel was poured using gradient mixer. Both 8% and 10% acrylamide solutions were made up using Tricine gel buffer (1 M Tris-Cl, pH 8.45, 0.1% [w/v] SDS) with 13% [v/v] glycerol added to the 10% mix and overlayed with a 4% stacker gel. Mitochondrial samples were boiled in SDS-PAGE loading dye (2X; 10 mM Tris-C, pH 6.8, 200 mM dithiothreitol, 4% [w/v] SDS, 20% [w/v] glycerol, 0.2% [w/v] bromophenol blue) before loading. Electrophoresis was performed using Tricine cathode buffer (0.1 M Tris, 0.1 M Tricine, pH 8.45, 0.1% SDS) and anode buffer (0.2 M Tris-Cl, pH 8.9). Gels were transferred onto 0.45 µM PVDF membrane (Millipore) using a semidry transfer apparatus prior to immunoblotting with mouse monoclonal SDHA primary antibody (Abcam: Ab14715, RRID: AB_301433) or rabbit polyclonal CLPB primary antibody (Abcam: Ab235349, RRID: AB_2847899) followed by secondary antibodies. Proteins were detected using Clarity Western ECL Substrate (Bio-Rad) on a ChemiDoc MP imaging machine (Bio-Rad). Quantification of bands was performed according to the manufacturer's instructions using the Image Lab software (Bio-Rad).

Results

WES Identifies Compound Heterozygous CLPB Variants

The patient was referred to our research program after pediatric endocrinology assessment and a diagnosis of POI at age 15 years with an elevated FSH of 73 IU/L. Further clinical details were not communicated at this time and initial data analysis was performed on the assumption that she suffered isolated POI.

Median exonic depth of coverage was 69× with > 95% of bases having a depth of greater than 10. There were 152 moderate-high priority variants detected in the exome of the patient that were further filtered to identify the likely causative genetic defect (Fig. 1A).

For gene-centric analysis, 9 missense variants in candidate POI genes were considered (Fig. 1A). These were discounted because their frequency in public databases was too high to cause POI in heterozygous state, the variants were predicted benign by online algorithms and/or were inherited from the unaffected mother.

For variant-centric analysis, only 1 gene was detected with recessive-type variants, *CDK5RAP1* (Fig. 1A). This gene was not considered likely causative as it has no known link to ovarian biology. Next, high-priority variants in any gene were considered. This revealed 9 predicted loss-of-function variants, including a paternally inherited previously reported pathogenic variant in *CLPB*, NM_030813.6:c.1249C>T, p.Arg417Ter (Fig. 2B) (5, 6). Given *CLPB* variants are associated with autosomal recessive 3-MGA-uria Type VII (OMIM: 616271) characterized by cataracts, neurologic involvement, and neutropenia, which did not match the presumed isolated POI of the patient, this heterozygous variant was initially dismissed.

WES data, however, were revisited upon clinical update of the patient phenotype to include congenital neutropenia, multiple infections, intellectual disability (IQ 58), eczema, asthma, bilateral cataracts, myopia, in addition to POI, making the heterozygous *CLPB* variant highly relevant. Given that CLPB deficiency is an autosomal recessive condition, we broadened our variant search using relaxed filters. We searched for any rare variant (<0.001 MAF) in *CLPB* including the intronic regions. This revealed a second *CLPB* variant, c.1257+5G>A (Fig. 1B). This variant was intronic but fell near the donor splice site for the exon 11/12 junction. The variant is absent in public databases, such as gnomAD, and the affected nucleotide is moderately conserved. The variant was maternally inherited, consistent with compound heterozygosity.

At the time of variant discovery, all reported cases of CLPB deficiency presented with urinary 3-MGA-uria. 3-MGA is a nonspecific hallmark of many syndromes with compromised mitochondrial function (30). In contrast to the previously reported patients with CLPB deficiency, no increased urinary excretion of 3-MGA was detected in the patient of this study.

A Novel CLPB Variant Causes Aberrant mRNA Splicing

The location of the maternally inherited c.1257+5G>A variant near a donor splice site raised the possibility of it disrupting gene splicing. SpliceAI predicted that this variant would break the wild-type donor site with a score of 0.51

A

	Median depth	69	
	% bases >x10	95.1	
	Mod-high priority (all)	152	
Gene-centric	Mod-high priority (POI)	9	*UBR4, IGFBP7, TRIM56, WRN, CACNA1H, BANP, TRPV3, NLRP5, PCNT*
Variant-centric	Bi-allelic (all)	1	*CDK5RAP1*
	High priority (all)	9	*NFYC, STK32B, ZAN, **CLPB***, EPYC, INF2, TPPP3, NPHS1, TCEANC*

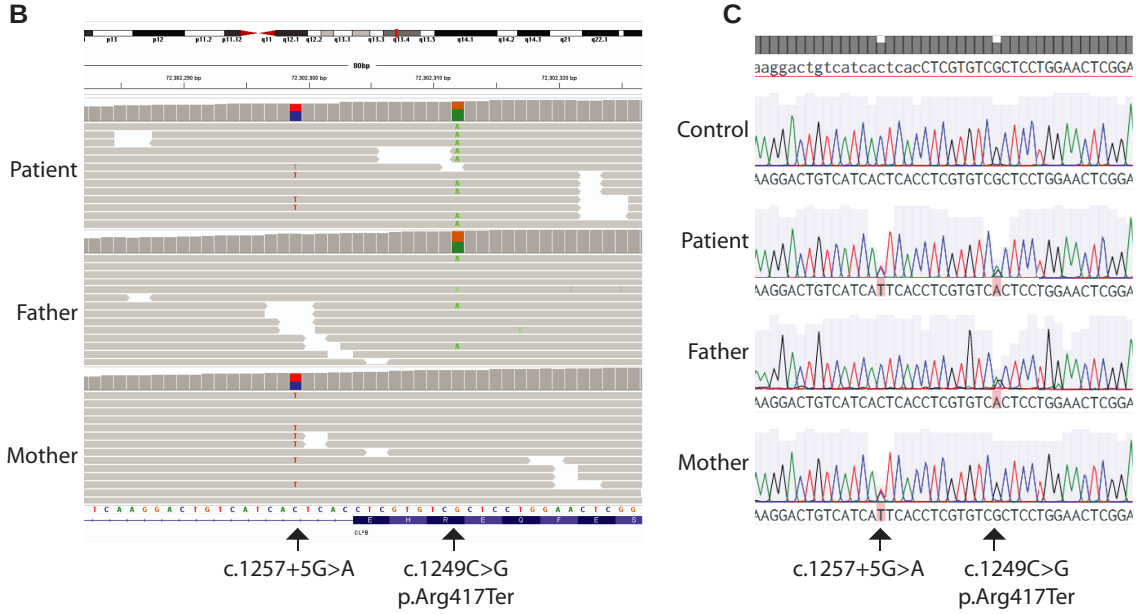

Figure 1. Whole-exome sequencing and variant filtration identifies compound heterozygous *CLPB* variants. (A) Variant filtration table showing results for standard gene-centric and variant-centric analysis. Initial data analysis identified only 1 *CLPB* variant, with the second variant identified by relaxation of filters. (B) IGV-snapshot of WES data indicates the c.1257+5G>A variant is maternally inherited and the c.1249C>T, p.Arg417Ter variant is paternally inherited.

(https://spliceailookup.broadinstitute.org/). Splice Site Prediction by Neural Network via the Berkeley Drosophila Genome Project (https://www.fruitfly.org/seq_tools/splice.html) similarly predicted the variant would impair splicing with the variant reducing the splicing prediction from 1.00 to 0.86.

To investigate whether the c.1257+5G>A affects *CLPB* mRNA splicing, RNA from patient lymphoblasts was analyzed using RT-PCR. RT-PCR amplification of a region encompassing exons 9 to 13 of *CLPB* demonstrated aberrant splicing with 3 transcripts detected. These corresponded to (1) use of a cryptic donor site introducing intronic sequence leading to a frameshift, (2) full-length transcript and (3) complete skipping of exon 11, likely leading to an in-frame loss of 15 amino acids (Fig. 2A and B).

To investigate the relative abundance of the alternative splice forms, RNAseq was performed on patient and control lymphoblast RNA. First, this demonstrated that the major *CLPB* isoform detected in lymphoblasts is isoform 2 (NM_001258392.2, Q9H078-2) which lacks Exon 5 of the canonical reference transcript. According to GTEx (https://gtexportal.org), the major *CLPB* isoform expressed in human lymphoblasts is the same as that expressed in ovarian tissue, suggesting insights into *CLPB* splicing in lymphoblasts will likely be relevant to ovarian development/function. Gene-focused RNAseq analysis revealed clear disruption of Exon 11 splicing with low exonic coverage compared to controls as well as coverage across the upstream and downstream flanking introns, indicating intronic retention. The majority (67%) of the reads across the site of the premature stop codon (PTC) (p.Arg417*) are wild-type, indicating that the majority of them are from the splicing allele and that transcripts containing the PTC are being degraded by nonsense-mediated decay (NMD). In contrast, 79% of the reads over the c.1257+5 site contain the splice variant, indicating that the majority of intron retention is due to the splicing variant. The splice variant clearly disrupts *CLPB* splicing with nearly all reads corresponding to skipping of exon 11 and very few reads with wild-type splicing and predicted to encode wild-type CLPB (only 4% of reads covering this region). The skipped exon encodes amino acids that lie between the Walker A motif and the Pore Loop, and loss may impair ATP binding.

An Additional Patient With Comparable CLPB Variants

Through international collaboration, we identified a patient (SCNIR-2735) with almost identical variants enrolled in the Severe Chronic Neutropenia International Registry

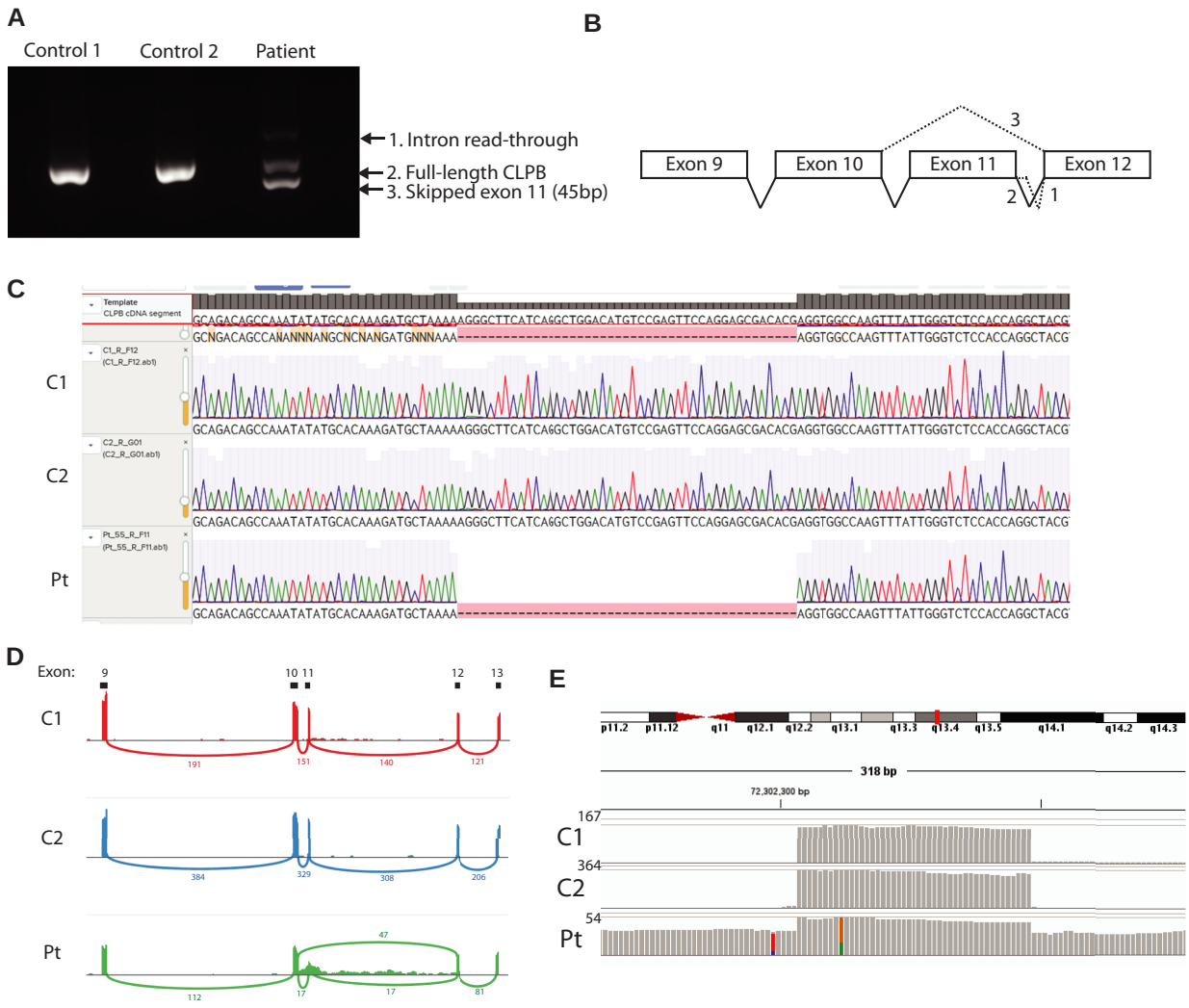

Figure 2. The novel c.1257G>A variant disrupts *CLPB* mRNA splicing. (A) RT-PCR of RNA extracted from patient lymphoblasts shows alternative splicing of *CLPB mRNA* with multiple splice species visible by gel electrophoresis. (B) Schematic representation of the alternative splicing observed in (A), with 3 major splice products corresponding to (1) use of a cryptic splice site and leading to intron retention, (2) residual wild-type splicing and (3) skipping of exon 11. (C) Sequencing of RT-PCR products demonstrates the major splice species lacks exon 11 (45 bp). (D) Sashimi plot generated from RNAseq data from patient lymphoblasts demonstrates skipping of exon 11, residual wild-type splicing and variable intron retention due to inconsistent splicing. (E) RNA seq reads over exon 11 with clean splicing seen in two controls. The majority of mRNA products with intron retention contain the c.1257+5G>A, whereas the majority of mRNA species containing exon 11, harbor the c.1249C>T, p.Arg417Ter variant.

(https://severe-chronic-neutropenia.org/en) (Table 1). She shared the previously reported p.Arg417Ter variant, in trans with an alternative splice variant affecting the same base altered in the proband of this study, c.1257+5G>T. It is likely that this variant similarly affects *CLPB* splicing. Supporting a similar splicing defect, SpliceAI predicted loss of the donor splice site with a score of 0.57 and Splice Site Prediction by Neural Network via the Berkeley Drosophila Genome Project predicted loss in splicing efficiency from a score of 1.0 to 0.79. The patient is currently 3 years old and has hallmark features of CLPB deficiency including neutropenia and infantile cataracts. Consistent with mild CLPB deficiency syndrome, the patient had no evidence of developmental delay or neurological involvement, although she presented with severe congenital neutropenia with bone marrow myeloid maturation arrest and bilateral infantile cataracts. Her ovarian status is currently unknown and she was not available for further hormonal testing, which may have provided evidence of ovarian dysgenesis, for example by elevated FSH or reduced AMH. We can speculate that the splice variant in this individual may cause a similarly mild phenotype and she may survive to adulthood and experience POI, although more evidence is required to confirm this genotype:phenotype correlation. The ongoing involvement of endocrinologists/gynecologists in her care could be advised, for early detection of ovarian insufficiency and prompt management by HRT.

Proteomics Demonstrates Loss of CLPB Protein and Disruption to Mitochondrial Protein Homeostasis

To understand the impact that these variants have on the CLPB protein and mitochondrial function, we performed whole cell direct data-independent acquisition (dDIA) quantitative proteomics on patient and control lymphoblasts. The major CLPB isoform detected in lymphoblasts was isoform 2 (NM_001258392.2, Q9H078-2) which lacks Exon 5 of

the canonical reference transcript, in keeping with RNAseq data. Unfortunately, no peptide corresponding to the predicted internal deleted region could be detected in the dDIA data, so we could not distinguish full-length CLPB from the CLPB variant protein generated by exon skipping. The data do, however, demonstrate a significantly low level of CLPB protein in patient lymphoblasts. The abundance of individual CLPB peptides upstream of the nonsense variant is higher than the level of individual peptides derived from sequence C-terminal of the nonsense variant. This suggests that the residual CLPB protein likely consists of truncated CLPB due to the nonsense variant on the paternal allele in addition to CLPB with or without an internal deletion from the maternal allele. The overall low level of CLPB protein indicates that the in-frame deletion due to exon skipping likely renders the protein unstable with rapid turnover (Fig. 3A). We also investigated CLPB protein level in mitochondria isolated from control and patient lymphoblasts by Western blot (Fig. 3B). Upon quantification, we found levels of mature CLPB in patient lymphoblasts to be significantly reduced in comparison to controls (Fig. 3C). CLPB in patient lymphoblasts appears to be migrating slightly slower than in control samples; however, the cause of this shift is not clear. There was no evidence of truncated CLPB, likely due to nonsense-mediated decay of the PTC-containing mRNA and sensitivity limitations of the CLPB antibody.

To investigate the biological consequence of CLPB disruption, comparative analysis between patient and control lymphoblast protein abundance was performed. The mitochondrial complement was filtered from the whole cell proteomic dataset and normalized independently. To discern those proteins significantly enriched or depleted from patient replicates, a two-sided *t* test was utilized, and results were visually represented as volcano plots (Fig. 3D). CLPB is significantly reduced in both whole cell and mitochondrial analyses, with a Log_2 fold difference of 1.90—a 3.73-fold reduction from control basal levels. Whole cell analysis (Fig. 3D, left) found increased abundance of proteins involved in B-cell differentiation and receptor signaling such as IGLL5, FCRLA, and MNDA. T-cell leukemia/lymphoma protein 1A (TCL1A) was also significantly increased in abundance, which mediates AKT1/2/3 phosphorylation and so enhances cell proliferation and survival by association (31). Though not mitochondrial itself, TCL1A phosphorylase activity is also important in stabilizing mitochondrial inner membrane potential (31). Significantly depleted relative to controls are multiple proteins involved in actin and cytoskeleton modification, as well as cell migration mechanisms, such as PFN2, MICAL3, CNN3, and INPP5F (Fig. 3D).

Proteins such as ENDOG, BAK1, and HAX1 are significantly increased in mitochondria from patient lymphoblasts relative to control (Fig. 3D, right). Overabundance of these proteins may reflect apoptotic vulnerability in cells lacking functional CLPB (32, 33) and compromised inner membrane potential (34). Proteins involved in lipid metabolism, such as ACADS, FDXR, APOL2, DHRS1, and AMACR, are depleted in patient lymphoblast mitochondria, indicating possible disruption to mitochondrial membrane maintenance.

Notably, there was no reduction in abundance of oxidative phosphorylation (OXPHOS) components (Fig. 3E). These data indicate that she does not have a primary OXPHOS deficiency, at least in this cell type. Instead, reduced amounts of functional CLPB may disrupt UPR^{MT} and sensitize cells to apoptotic induction, but further work is needed to clarify the mechanisms underscoring mitochondrial dysfunction in CLPB deficiency.

Premature Ovarian Insufficiency Is a Consistent Component of "Mild" CLPB Deficiency

CLPB deficiency clearly explained the neutropenia, intellectual disability, cataracts, and recurrent infections of our patient; however, the role of CLPB in ovarian functioning is not well established. Close examination of the literature revealed that POI was mentioned in a case described by Kanabus et al (35) and one of the milder cases described by Wortman et al had "hypergonadotropic hypogonadism" (6). This phrase is interchangeable with POI as it is also defined by elevated gonadotropin (FSH) and low ovarian activity. Finally, one of the carriers of a heterozygous *CLPB* variant causing severe congenital neutropenia is also listed as having POI (9). Patients with severe congenital neutropenia due to deficiency of HAX1, which is a known interactor of CLPB, also experience gonadal failure (36). The majority of patients with biallelic *CLPB* variants reported to date, however, have not survived beyond childhood and/or have not reached pubertal age before reporting, consistent with a bias toward severe early-onset presentation for initial publications. Indeed, carriers of the more recently described dominant *CLPB* pathogenic variants tend to survive to adulthood (9). It seems likely that POI is a consistent feature of CLPB deficiency in postpubertal females.

To explore this possibility, we obtained updated information on patients with CLPB deficiency who have survived to adulthood. As suspected, this revealed that POI is commonly experienced by postpubertal females with CLPB deficiency (Table 1). Of note, male fertility is likely also affected by CLPB deficiency with oligospermia/azoospermia reported in postpubertal males (Table 1).

Discussion

A Novel Splicing Variant in CLPB Provides Further Insight into Genotype: Phenotype Correlation

Variants in *CLPB* are known to cause a mitochondrial disorder with variable severity (5-8, 35, 37). Typically, patients present in infancy with progressive encephalopathy and elevated urinary 3-MGA. Other common features include cataracts, seizures, neutropenia, and recurrent infections. In most reported cases, the disease course is severe, leading to neonatal or infantile death. Despite this being the most frequently described presentation, there are cases of milder disease. Some individuals survive childhood and have a phenotype consisting of neutropenia, movement disturbance due to hypotonia and/or spasticity, epilepsy, and/or intellectual disability (6). The mildest cases described have no neurological involvement, and present with cataracts with or without nephrocalcinosis or congenital neutropenia (35).

It appears that there is genotype:phenotype correlation with respect to variants in this gene (38). Patients with biallelic loss-of-function variants tend to present with severe and lethal disease, whereas individuals with biallelic missense variants tend to present with milder disease and survival beyond childhood. Recently it has been discovered that heterozygous missense variants affecting the C-terminal

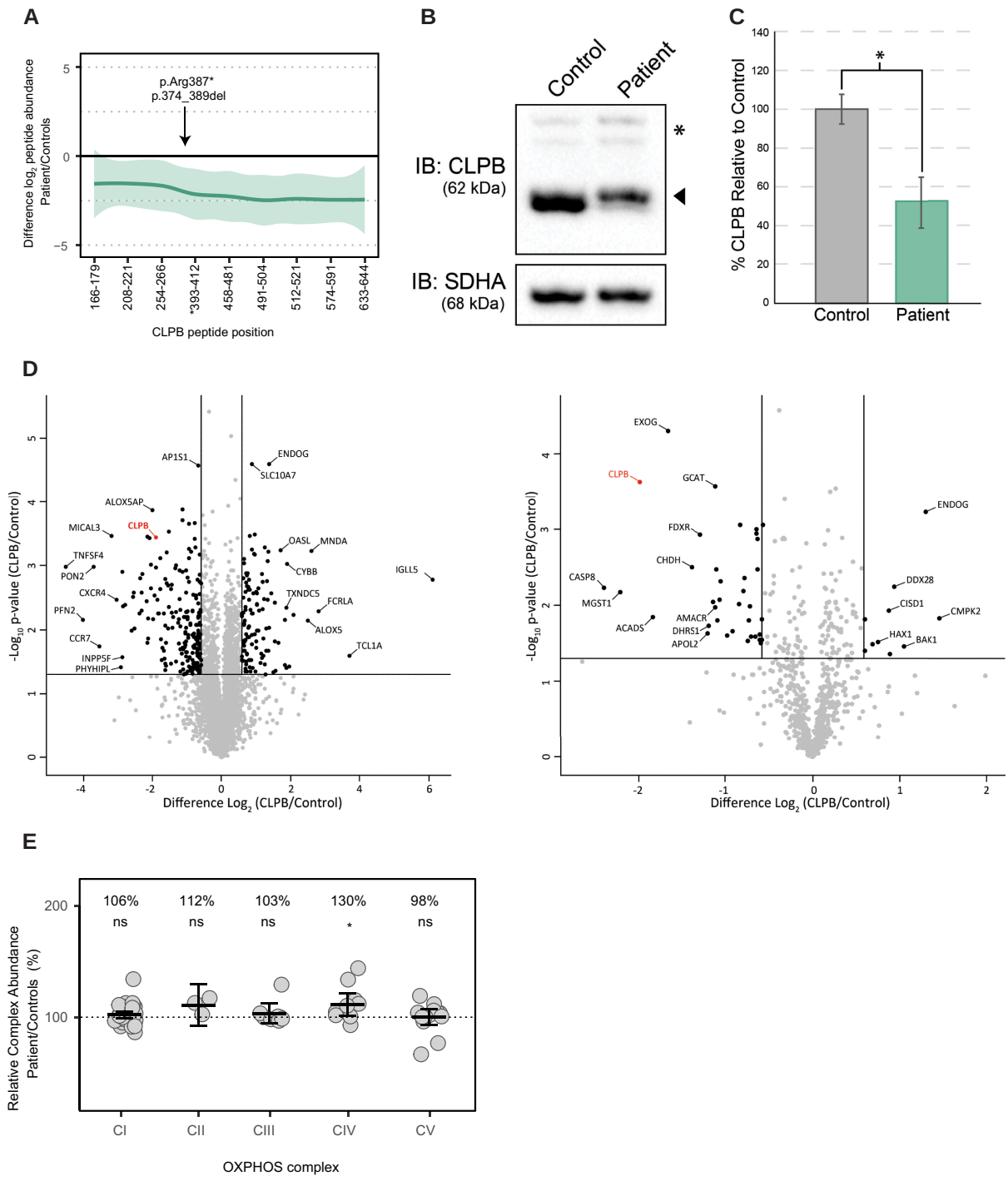

Figure 3. Proteomics of patient lymphoblasts demonstrate CLPB deficiency and its biological consequences (A) Relative peptide abundance across CLPB protein in the patient compared to controls from whole-cell lymphoblast quantitative proteomics. The mean difference of $\log_2$ MS2 intensities between the patient to controls (n = 2) was plotted for individual peptides across the most common CLPB protein (isoform 2, NP_001245321.1) using loess smoothed curve along with the 95% confidence interval. Missing values in the patient for a single peptide (*) were imputed with the lowest CLPB peptide level detected. The CLPB patient variants were adapted to CLPB isoform 2. (B) Mitochondria were isolated from control and patient lymphoblasts and analyzed by SDS-PAGE on low percentage (10%) acrylamide gel to resolve alternative processing of CLPB protein. Filled arrow indicates mature CLPB bands, asterisk indicates nonspecific banding. (C) The relative level of mature CLPB was quantified and normalized with respect to SDHA loading control, and graphed as average ± SD, (n = 3). Statistical significance was determined by two-sided *t* test: * $P < 0.05$. (D) Whole cell dDIA proteomics [LEFT] and filtered mitochondrial component [RIGHT] volcano plots showing relative levels of whole cell/mitochondrial proteins within patient compared to control lymphoblasts. Black dots beyond the vertical lines represent proteins with significant fold change in the patient cell line compared to controls, with significance denoted by *P* value following a two-sample Student *t* test (*P* value <0.05, fold change ±1.5). n = 3 patient replicates and n = 2 independent control replicates. (E) Relative complex abundance (RCA) of OXPHOS complexes in lymphoblasts from CLPB patient relative to controls (n = 2). The middle bar represents the mean complex abundance, upper and lower bars represent 95% confidence interval of the mean. * = $P \leq 0.05$, ns = not significant calculated from a paired *t* test.

ATP-binding domain of the protein cause nonsyndromic severe congenital neutropenia (9).

Our patient harbors one nonsense variant that has previously been reported in cases of severe disease when in trans with another loss-of-function allele, or in cases of moderate disease when in trans with a missense allele (8). The second allele in our patient carried an intronic variant in the vicinity of a canonical donor site. Splice site variants affecting the canonical dinucleotides (GT for donor sites and AG for acceptor sites) are usually predicted loss-of-function alleles. The consequence of variants affecting the neighboring bases, however, is more difficult to predict. Given the patient's survival to adulthood and the proposed genotype:phenotype correlation with respect to variants in this gene, we predicted that the variant did not cause complete loss-of-function. To investigate the consequence of the variant, we performed transcriptomics and proteomics. This revealed that the patient did indeed have a splicing defect and at least 3 *CLPB* mRNA species could be distinguished in patient RNA. These transcripts encoded truncated CLPB (as a consequence of the nonsense allele), CLPB with an in-frame deletion of 15 amino acids (due to exon skipping), and very low residual wild-type CLPB protein (due to occasional wild-type splicing). Although exon skipping generated a somewhat robust splice product, proteomics revealed a very low level of CLPB protein, indicating that protein with the in-frame deletion is likely unstable and turned over rapidly. The survival of this patient beyond childhood may be due to residual function of CLPB with the in-frame deletion and/or wild-type protein generated by the occasional wild-type splicing that is preserved despite the c.1257+5G>A variant. The former may be considered the more likely explanation given the very low (almost negligible) abundance of wild-type transcript.

We have described the first causative splicing variants in *CLPB*. RNA and protein analysis supports this being a "milder" allele, likely allowing survival of the patient beyond childhood and providing further evidence of the genotype: phenotype correlation with respect to variants in this gene.

The Role of CLPB and Mitochondria for Ovarian Function

CLPB encodes caseinolytic peptidase B homolog CLPB, which is a member of the family of AAA+-ATPases associated with diverse cellular activities. It localizes to the mitochondria where it is believed to regulate protein folding including the disaggregation of misfolded proteins (4). The mitochondrial unfolded protein response (UPR^{MT}) is activated when mitochondrial function is compromised, and its role is to repair and recover the mitochondrial network. For example, UPR^{MT} promotes recovery from mitochondrial dysfunction due to toxins, pathogens, or genetic variants disrupting the respiratory chain (39, 40). These stressors lead to misfolded proteins that trigger the upregulation of proteases, such as CLPB and CLPP (41, 42) that then disaggregate and cleave misfolded proteins, respectively. Cleaved proteins can activate a transcriptional program that promotes mitochondrial biogenesis/function and cell survival during stress (43, 44). Prolonged or excessive activation of the UPR^{MT}, however, can lead to the accumulation of aberrant mitochondrial genomes that contribute to aging pathology (45, 46). The level of UPR^{MT} therefore needs to be tightly regulated. Disruption of UPR^{MT} can cause severe mitochondrial dysfunction and oocyte damage. For example, deletion of the protease *Clpp* in mice leads to mitochondrial dysfunction, accelerated oocyte depletion, and female infertility (47). Similarly, pathogenic variants in *CLPP* cause the human condition, Perrault syndrome, characterized by POI with sensorineural hearing loss (48). Whether CLPB acts directly in the classical UPR^{MT} response or regulates the mitochondrial proteome via another means remains to be established. Our current study highlights, however, that disruption of the mitochondrial proteome via CLPB deficiency affects ovarian function.

The importance of mitochondria to ovarian development and function is manifold. Mitochondria, being the powerhouse of cells, provide the energy required for the high-demand activities of the ovaries. For example, energy is needed to support large-scale oocyte proliferation during ovarian development, for the expansion of follicles to greater than 500 times their original size during folliculogenesis, and for continuous transcription and translation within oocytes during their maturation. Reactive oxygen species (ROS) are a by-product of mitochondrial energy generation and can accumulate when mitochondria are defective. This leads to oxidative stress that can cause oocyte damage and follicular atresia (49), leading to POI.

Given that mitochondria supply cellular energy for all bodily functions, it is not surprising that mitochondrial disorders are usually multiorgan syndromes with involvement of organs with high energy demand such as the brain, heart, muscle, liver, and/or kidneys. Mitochondrial disorders are often fatal in childhood but milder forms allow survival to adulthood (50). There are a number of mitochondrial disease genes that have been found to cause milder adult-onset disease, and POI is a common feature of such conditions. Examples include POI in association with sensorineural hearing loss due to variants in *TFAM* (51, 52), *LARS2* (53), *HARS2* (54), *ERAL1* (55), *CLPP* (48), or *TWNK* (56); POI in association with adult-onset neurodegeneration due to variants in *AARS2* (57) or *LARS2* (58); or POI in association with vision loss or parkinsonism due to variants in *TWNK* (59, 60). Many of these genes were first identified in association with severe pediatric disease such as neonatal liver failure in the case of *TFAM* (61) or fatal infantile hypertrophic cardiomyopathy in the case of *AARS2* (62). This is consistent with an early research bias toward severe disease. As WES studies become more frequent and knowledge of genetic disease expands, milder conditions are gaining research attention. Our study sheds light on the long-term consequence of mild CLPB deficiency, highlighting that POI is a major feature of this syndrome that should be considered in affected individuals. It is likely that there are further undiagnosed cases whose endocrinological manifestations will be important to manage.

It is interesting to note that 40% (4/10) of parents of patients with severe CLPB deficiency and 17% (2/12) of parents of patients with moderate disease have reported difficulty conceiving (8). It has been proposed that this could be due to embryonic lethality of *CLPB* deficiency. Our study highlights an alternative possibility, that maternal haploinsufficiency of CLPB may cause mild mitochondrial disruption that results in reduced oocyte integrity and subfertility. Interestingly, a recent analysis of WES data from 132 370 women found that *CLPB* was one of 2 genes in which rare and damaging variants are associated with earlier menopause. Furthermore, an enrichment of rare and damaging *CLPB* variants were identified within 2074 women with POI (63). Given that POI has not been well-described in CLPB deficiency in the literature, the

authors considered the gene to lack prior evidence linking it to menopause. The association data, however, support the requirement of CLPB for ovarian function and the potential for *CLPB* variants to impact fertility.

The Importance of Complete and Accurate Phenotypic Information for WES Data Analysis

The initial clinical information received about this patient related only to her ovarian function. Gene-centric WES analysis, therefore, focused on candidate POI genes and did not include targeted analysis of the *CLPB* gene. Variant-centric analysis failed to identify biallelic variants in *CLPB* because the second variant did not affect exonic sequence or canonical splice sites. Pathogenic variant detection required full phenotype description that prompted relaxation of filters and targeted analysis of the *CLPB* gene, including flanking intronic sequences. This underscores the importance of complete and accurate clinical information, and broad genetic understanding for variant curation. As genetic syndromes are increasingly being recognized and known phenotypic spectra are broadening, cross-disciplinary communication is particularly important so that apparently independent symptoms can accurately be tied together through unifying genetic diagnoses.

Recognizing POI as a Feature of CLPB Deficiency: Improved Patient Management

Although the proband of this study presented in early adolescence with growth deficiency and early recognition of pubertal delay, the syndromic nature of CLPB deficiency and the burden of other symptoms means that lack of menarche may often be overlooked by patients and their families and not acted upon until much later, delaying HRT. The involvement of endocrinological abnormalities in patients with mitochondrial disorders surviving to adulthood has implication for their long-term health and wellbeing. Individuals with mild disease may desire future fertility. Early identification of POI provides opportunity for intervention such as cryopreservation of eggs before their depletion. POI not only causes infertility, but also elevates risk of comorbidities, including osteoporosis, diabetes, heart disease, and early mortality (16-18). Prompt recognition of POI enables early treatment with HRT, which can provide protection against future disease. For example, early intervention with hormone replacement therapy increases bone density and reduces the risk of coronary heart disease and mortality (21, 22). Having established that POI is a common condition suffered by patients with CLPB deficiency, engagement with an appropriate health care team including a pediatric endocrinologist/gynecologist would be recommended for optimal patient management and outcomes. Of note, the neutropenia in CLPB patients has been reported to progress to myelodysplastic syndrome and leukemia in some individuals (6, 9, 10). The long-term outcomes of patients with CLPB deficiency may also be improved by the involvement of oncologists who can conduct surveillance for the early detection of cancer.

Conclusion

In summary, the current work describes a novel splicing variant in trans with a previously reported *CLPB* variant in an individual who presented with premature ovarian insufficiency in association with neutropenia, cataracts, and intellectual disability. A second patient with nearly identical variants in trans is also described. We validate that these variants disrupt *CLPB* mRNA and protein, leading to disrupted mitochondrial proteostasis. We establish that POI is a frequent manifestation of CLPB deficiency in female patients who survive to puberty. This work sheds light on the long-term consequences of CLPB deficiency, recognition of which can improve patient management and outcomes.

Acknowledgments

The research conducted at the Murdoch Children's Research Institute was supported by the Victorian government's operational infrastructure support program. We acknowledge the Bio21 Mass Spectrometry and Proteomics Facility (MMSPF) for the provision of instrumentation, training, and technical support.

Funding

This work was supported by an National Health and Medical Research Council (NHMRC) program grant (1074258 to A.H.S.), NHMRC grant (1140906 to D.A.S.), NHMRC fellowships (1054432 to E.J.T., 1126995 to R.S., 2009732 to D.A.S., 1062854 to A.H.S.), a Suzi Carp postdoctoral scholarship (to E.J.T.), a CHU Rennes grant (Appel à Projets Innovations 2019 to S.J.), an Australian Government Research Training Program scholarship (to M.J.B.), the Australian Mito Foundation for provision of instrumentation, incubator grants (to E.J.T. and D.S.), a Booster grant (to D.S.) and PhD Top-up scholarships (to M.J.B. and D.H.H.), and a Medical Research Council (UK) Clinician Scientist Fellowship (MR/S002065/1 to R.D.S.P.). S.B.W. was funded by ERAPERMED2019-310—Personalized Mitochondrial Medicine (PerMiM): Optimizing diagnostics and treatment for patients with mitochondrial diseases (FWF 4704-B).

Disclosure

The authors have nothing to disclose.

Data Availability

Some or all datasets generated during and/or analyzed during the current study are not publicly available but are available from the corresponding author on reasonable request.

References

1. Nargund AM, Pellegrino MW, Fiorese CJ, Baker BM, Haynes CM. Mitochondrial import efficiency of ATFS-1 regulates mitochondrial UPR activation. *Science*. 2012;337(6094):587-590.
2. Pimenta de Castro I, Costa AC, Lam D, *et al.* Genetic analysis of mitochondrial protein misfolding in Drosophila melanogaster. *Cell Death Differ*. 2012;19(8):1308-1316.
3. Runkel ED, Liu S, Baumeister R, Schulze E. Surveillance-activated defenses block the ROS-induced mitochondrial unfolded protein response. *PLoS Genet*. 2013;9(3):e1003346.
4. Cupo RR, Shorter J. Skd3 (human ClpB) is a potent mitochondrial protein disaggregase that is inactivated by 3-methylglutaconic aciduria-linked mutations. *Elife*. 2020;9:e55279.
5. Saunders C, Smith L, Wibrand F, *et al.* CLPB Variants associated with autosomal-recessive mitochondrial disorder with cataract, neutropenia, epilepsy, and methylglutaconic aciduria. *Am J Hum Genet*. 2015;96(2):258-265.

6. Wortmann SB, Zietkiewicz S, Kousi M, *et al.* CLPB Mutations cause 3-methylglutaconic aciduria, progressive brain atrophy, intellectual disability, congenital neutropenia, cataracts, movement disorder. *Am J Hum Genet*. 2015;96(2):245-257.
7. Capo-Chichi JM, Boissel S, Brustein E, *et al.* Disruption of CLPB is associated with congenital microcephaly, severe encephalopathy and 3-methylglutaconic aciduria. *J Med Genet*. 2015;52(5):303-311.
8. Pronicka E, Ropacka-Lesiak M, Trubicka J, *et al.* A scoring system predicting the clinical course of CLPB defect based on the foetal and neonatal presentation of 31 patients. *J Inherit Metab Dis*. 2017;40(6):853-860.
9. Warren JT, Cupo RR, Wattanasirakul P, *et al.* Heterozygous variants of CLPB are a cause of severe congenital neutropenia. *Blood*. 2021;139(5):779.
10. Wortmann SB, Zietkiewicz S, Guerrero-Castillo S, *et al.* Neutropenia and intellectual disability are hallmarks of biallelic and de novo CLPB deficiency. *Genet Med*. 2021;23(9):1705-1714.
11. Chiang JL, Shukla P, Pagidas K, *et al.* Mitochondria in ovarian aging and reproductive longevity. *Ageing Res Rev*. 2020;63:101168.
12. Shoubridge EA, Wai T. Mitochondrial DNA and the mammalian oocyte. In: St. John J, ed. *The Mitochondrion in the Germline and Early Development* 2007:87-111.
13. Tarin JJ, Vendrell FJ, Ten J, Blanes R, van Blerkom J, Cano A. The oxidizing agent tertiary butyl hydroperoxide induces disturbances in spindle organization, c-meiosis, and aneuploidy in mouse oocytes. *Mol Hum Reprod*. 1996;2(12):895-901.
14. Choi WJ, Banerjee J, Falcone T, Bena J, Agarwal A, Sharma RK. Oxidative stress and tumor necrosis factor-alpha-induced alterations in metaphase II mouse oocyte spindle structure. *Fertil Steril*. 2007;88(4 Suppl):1220-1231.
15. Tiosano D, Mears JA, Buchner DA. Mitochondrial dysfunction in primary ovarian insufficiency. *Endocrinology*. 2019;160(10):2353-2366.
16. Tao XY, Zuo AZ, Wang JQ, Tao FB. Effect of primary ovarian insufficiency and early natural menopause on mortality: a meta-analysis. *Climacteric*. 2016;19(1):27-36.
17. Eastell R. Management of osteoporosis due to ovarian failure. *Med Pediatr Oncol*. 2003;41(3):222-227.
18. Anagnostis P, Christou K, Artzouchaltzi AM, *et al.* Early menopause and premature ovarian insufficiency are associated with increased risk of type 2 diabetes: a systematic review and meta-analysis. *Eur J Endocrinol*. 2019;180(1):41-50.
19. Tucker EJ, Grover SR, Bachelot A, Touraine P, Sinclair AH. Premature ovarian insufficiency: new perspectives on genetic cause and phenotypic spectrum. *Endocr Rev*. 2016;37(6):609-635.
20. Tucker EJ, Grover SR, Robevska G, van den Bergen J, Hanna C, Sinclair AH. Identification of variants in pleiotropic genes causing "isolated" premature ovarian insufficiency: implications for medical practice. *Eur J Hum Genet*. 2018;26(9):1319-1328.
21. Keck C, Taylor M. Emerging research on the implications of hormone replacement therapy on coronary heart disease. *Curr Atheroscler Rep*. 2018;20(12):57.
22. Podfigurna A, Maciejewska-Jeske M, Nadolna M, *et al.* Impact of hormonal replacement therapy on bone mineral density in premature ovarian insufficiency patients. *J Clin Med*. 2020;9(12):3961.
23. Wen J, Huang K, Du X, *et al.* Can inhibin B reflect ovarian reserve of healthy reproductive age women effectively? *Front Endocrinol (Lausanne)*. 2021;12:626534.
24. Sadedin SP, Dashnow H, James PA, *et al.* Cpipe: a shared variant detection pipeline designed for diagnostic settings. *Genome Med*. 2015;7(1):68.
25. Tucker EJ, Jaillard S, Grover SR, *et al.* TP63-truncating Variants cause isolated premature ovarian insufficiency. *Hum Mutat*. 2019;40(7):886-892.
26. Kim D, Langmead B, Salzberg SL. HISAT: a fast spliced aligner with low memory requirements. *Nat Methods*. 2015;12(4):357-360.
27. Katz Y, Wang ET, Silterra J, *et al.* Quantitative visualization of alternative exon expression from RNA-seq data. *Bioinformatics*. 2015;31(14):2400-2402.
28. Johnston AJ, Hoogenraad J, Dougan DA, *et al.* Insertion and assembly of human tom7 into the preprotein translocase complex of the outer mitochondrial membrane. *J Biol Chem*. 2002;277(44):42197-42204.
29. Schagger H, von Jagow G. Tricine-sodium dodecyl sulfate-polyacrylamide gel electrophoresis for the separation of proteins in the range from 1 to 100 kDa. *Anal Biochem*. 1987;166(2):368-379.
30. Wortmann SB, Kluijtmans LA, Rodenburg RJ, *et al.* 3-Methylglutaconic Aciduria–lessons from 50 genes and 977 patients. *J Inherit Metab Dis*. 2013;36(6):913-921.
31. Laine J, Kunstle G, Obata T, Sha M, Noguchi M. The protooncogene TCL1 is an akt kinase coactivator. *Mol Cell*. 2000;6(2):395-407.
32. Schafer P, Scholz SR, Gimadutdinow O, *et al.* Structural and functional characterization of mitochondrial EndoG, a sugar nonspecific nuclease which plays an important role during apoptosis. *J Mol Biol*. 2004;338(2):217-228.
33. Westphal D, Kluck RM, Dewson G. Building blocks of the apoptotic pore: how Bax and Bak are activated and oligomerize during apoptosis. *Cell Death Differ*. 2014;21(2):196-205.
34. Klein C, Grudzien M, Appaswamy G, *et al.* HAX1 Deficiency causes autosomal recessive severe congenital neutropenia (Kostmann disease). *Nat Genet*. 2007;39(1):86-92.
35. Kanabus M, Shahni R, Saldanha JW, *et al.* Bi-allelic CLPB mutations cause cataract, renal cysts, nephrocalcinosis and 3-methylglutaconic aciduria, a novel disorder of mitochondrial protein disaggregation. *J Inherit Metab Dis*. 2015;38(2):211-219.
36. Cekic S, Saglam H, Gorukmez O, Yakut T, Tarim O, Kilic SS. Delayed puberty and gonadal failure in patients with HAX1 mutation. *J Clin Immunol*. 2017;37(6):524-528.
37. Kiykim A, Garncarz W, Karakoc-Aydiner E, *et al.* Novel CLPB mutation in a patient with 3-methylglutaconic aciduria causing severe neurological involvement and congenital neutropenia. *Clin Immunol*. 2016;165:1-3.
38. Pronicka E, Piekutowska-Abramczuk D, Ciara E, *et al.* New perspective in diagnostics of mitochondrial disorders: two years' experience with whole-exome sequencing at a national paediatric centre. *J Transl Med*. 2016;14(1):174.
39. Pellegrino MW, Nargund AM, Kirienko NV, Gillis R, Fiorese CJ, Haynes CM. Mitochondrial UPR-regulated innate immunity provides resistance to pathogen infection. *Nature*. 2014;516(7531):414-417.
40. Callegari S, Dennerlein S. Sensing the stress: a role for the UPR(mt) and UPR(am) in the quality control of mitochondria. *Front Cell Dev Biol*. 2018;6:31.
41. Haynes CM, Petrova K, Benedetti C, Yang Y, Ron D. Clpp mediates activation of a mitochondrial unfolded protein response in C. elegans. *Dev Cell*. 2007;13(4):467-480.
42. Murdock DG, Boone BE, Esposito LA, Wallace DC. Up-regulation of nuclear and mitochondrial genes in the skeletal muscle of mice lacking the heart/muscle isoform of the adenine nucleotide translocator. *J Biol Chem*. 1999;274(20):14429-14433.
43. Aldridge JE, Horibe T, Hoogenraad NJ. Discovery of genes activated by the mitochondrial unfolded protein response (mtUPR) and cognate promoter elements. *PLoS One*. 2007;2(9):e874.
44. Benedetti C, Haynes CM, Yang Y, Harding HP, Ron D. Ubiquitin-like protein 5 positively regulates chaperone gene expression in the mitochondrial unfolded protein response. *Genetics*. 2006;174(1):229-239.
45. Lin YF, Schulz AM, Pellegrino MW, Lu Y, Shaham S, Haynes CM. Maintenance and propagation of a deleterious mitochondrial genome by the mitochondrial unfolded protein response. *Nature*. 2016;533(7603):416-419.

46. Shpilka T, Haynes CM. The mitochondrial UPR: mechanisms, physiological functions and implications in ageing. *Nat Rev Mol Cell Biol*. 2018;19(2):109-120.
47. Wang T, Babayev E, Jiang Z, *et al*. Mitochondrial unfolded protein response gene clpp is required to maintain ovarian follicular reserve during aging, for oocyte competence, and development of pre-implantation embryos. *Aging Cell*. 2018;17(4):e12784.
48. Jenkinson EM, Rehman AU, Walsh T, *et al*. Perrault syndrome is caused by recessive mutations in CLPP, encoding a mitochondrial ATP-dependent chambered protease. *Am J Hum Genet*. 2013;92(4):605-613.
49. Wang L, Tang J, Wang L, *et al*. Oxidative stress in oocyte aging and female reproduction. *J Cell Physiol*. 2021;236(12):7966-7983.
50. Chinnery PF. Mitochondrial disease in adults: what's Old and what's New? *EMBO Mol Med*. 2015;7(12):1503-1512.
51. Tucker EJ, Rius R, Jaillard S, *et al*. Genomic sequencing highlights the diverse molecular causes of Perrault syndrome: a peroxisomal disorder (PEX6), metabolic disorders (CLPP, GGPS1), and mtDNA maintenance/translation disorders (LARS2, TFAM). *Hum Genet*. 2020;139(10):1325-1343.
52. Ullah F, Rauf W, Khan K, *et al*. A recessive variant in TFAM causes mtDNA depletion associated with primary ovarian insufficiency, seizures, intellectual disability and hearing loss. *Hum Genet*. 2021;140(12):1733-1751.
53. Pierce SB, Gersak K, Michaelson-Cohen R, *et al*. Mutations in LARS2, encoding mitochondrial leucyl-tRNA synthetase, lead to premature ovarian failure and hearing loss in Perrault syndrome. *Am J Hum Genet*. 2013;92(4):614-620.
54. Pierce SB, Chisholm KM, Lynch ED, *et al*. Mutations in mitochondrial histidyl tRNA synthetase HARS2 cause ovarian dysgenesis and sensorineural hearing loss of Perrault syndrome. *Proc Natl Acad Sci U S A*. 2011;108(16):6543-6548.
55. Chatzispyrou IA, Alders M, Guerrero-Castillo S, *et al*. A homozygous missense mutation in ERAL1, encoding a mitochondrial rRNA chaperone, causes Perrault syndrome. *Hum Mol Genet*. 2017;26(13):2541-2550.
56. Morino H, Pierce SB, Matsuda Y, *et al*. Mutations in Twinkle primase-helicase cause Perrault syndrome with neurologic features. *Neurology*. 2014;83(22):2054-2061.
57. Dallabona C, Diodato D, Kevelam SH, *et al*. Novel (ovario) leukodystrophy related to AARS2 mutations. *Neurology*. 2014;82(23):2063-2071.
58. van der Knaap MS, Bugiani M, Mendes MI, *et al*. Biallelic variants in LARS2 and KARS cause deafness and (ovario)leukodystrophy. *Neurology*. 2019;92(11):e1225-e1237.
59. Luoma P, Melberg A, Rinne JO, *et al*. Parkinsonism, premature menopause, and mitochondrial DNA polymerase gamma mutations: clinical and molecular genetic study. *Lancet*. 2004;364(9437):875-882.
60. Pagnamenta AT, Taanman JW, Wilson CJ, *et al*. Dominant inheritance of premature ovarian failure associated with mutant mitochondrial DNA polymerase gamma. *Hum Reprod*. 2006;21(10):2467-2473.
61. Stiles AR, Simon MT, Stover A, *et al*. Mutations in TFAM, encoding mitochondrial transcription factor A, cause neonatal liver failure associated with mtDNA depletion. *Mol Genet Metab*. 2016;119(1-2):91-99.
62. Gotz A, Tyynismaa H, Euro L, *et al*. Exome sequencing identifies mitochondrial alanyl-tRNA synthetase mutations in infantile mitochondrial cardiomyopathy. *Am J Hum Genet*. 2011;88(5):635-642.
63. Ward LD, Parker MM, Deaton AM, *et al*. Rare coding variants in DNA damage repair genes associated with timing of natural menopause. *HGG Adv*. 2022;3(2):100079.